AIAA-2002-4256

A High-Speed Probe Positioning System for Interrogating the Discharge Plasma of a 30 cm Ion Thruster

Daniel A. Herman and Alec D. Gallimore
Plasmadynamics and Electric Propulsion Laboratory
University of Michigan
Ann Arbor, MI 48105 USA

38th AIAA/ASME/SAE/ASEE
Joint Propulsion Conference & Exhibit
7-10 July 2002
Indianapolis, Indiana

For permission to copy or republish, contact the copyright owner named on the first page.
For AIAA-held copy write, write to AIAA Permissions Department,
1801 Alexander Bell Drive, Suite 500, Reston, VA 20191-4344.

A High-Speed Probe Positioning System for Interrogating the Discharge Plasma of a 30 cm Ion Thruster

Daniel A. Herman* and Alec D. Gallimore†
Plasmadynamics and Electric Propulsion Laboratory
University of Michigan
Ann Arbor, MI 48105 USA

Abstract

A method for delivery of a symmetric double probe into the discharge chamber of a 30-cm diameter ring-cusped ion thruster is discussed. Motivation for direct access of the electrostatic probe to the discharge chamber stems from the need to characterize the discharge plasma to better understand the possible cause of discharge cathode assembly (DCA) erosion. A symmetric double probe allows electron temperature and number density measurements with minimal perturbation to the discharge plasma and thruster operating conditions. The High-speed Axial Reciprocating Probe positioning system (HARP) was used to further minimize thruster perturbation during probe insertion and minimize heating of the probe. Integration issues and selection criteria for hardware used for interrogation of the discharge plasma are reviewed. Preliminary plasma parameters were measured 2.6 mm downstream of the keepered DCA at various discharge cathode operating conditions. The electron number density was found to range from $8.9 \times 10^{10} - 2.1 \times 10^{12}$ cm^{-3} with the maximum occurring at DCA centerline for each operating condition. Electron temperature ranged from 3.2 – 4.8 eV, consistent with predictions for ion thrusters incorporating a ring-cusped design. Improvements for increasing the accuracy of future mappings of the discharge plasma are suggested.

Nomenclature

A_p	Probe surface area, m^2	P_i	Indicated pressure (with xenon flow), Torr
e	Electron charge, 1.6×10^{-19} C	P_c	Corrected pressure (on xenon), Torr
$i_{ion,sat}$	Ion saturation current, A	T_e	Electron temperature, eV
I_a	Acceleration grid current, mA	V_d	Discharge voltage, V
I_b	Beam current, A	V_g	Neutralizer to ground coupling voltage, V
I_d	Discharge current, A	V_s	Screen grid voltage, V
I_{nk}	Neutralizer keeper current, A	V_a	Acceleration grid voltage, V
k	Boltzmann's constant, 1.38×10^{-23} J/K	V_{nk}	Neutralizer keeper voltage, V
M_{Xe}	Atomic mass of xenon, kg	ϕ	Probe bias potential, V
n_e	Electron number density, m^{-3}		
P_b	Base pressure (air), Torr		

* Graduate Student, Student Member AIAA, hermo@engin.umich.edu.
† Associate Professor and Laboratory Director, Associate Fellow AIAA.

Copyright © 2002 by Daniel A. Herman.
Published by the American Institute of Aeronautics and Astronautics with permission.

Introduction

Ion thrusters are high efficiency, high specific impulse (I_{sp}) propulsion systems that have been proposed as the primary propulsion source for a variety of missions. The NASA Solar Electric Propulsion Technology Applications Readiness (NSTAR) 30 cm ion thruster was the first ion engine to be used for primary propulsion and has demonstrated operation for over three times its intended lifetime.[1] Although this places NSTAR as the record holder for the most hours of operation for an in-space thruster, efforts to further increase engine lifetime continue.

A potential failure mechanism for ion engine technology is erosion of the Discharge Cathode Assembly's (DCA) downstream surface.[2] In order to mitigate DCA erosion on NSTAR, an engineering solution of adding a cathode keeper electrode was employed.[3] This led to a decrease in DCA erosion and, until recently, was thought to have solved the DCA erosion issue. An ongoing Extended Life Test (ELT) of the flight spare thruster is being conducted at the Jet Propulsion Laboratory (JPL).[4] Extensive discharge cathode keeper erosion has been observed after 12,000 hours of testing, which has yet to be fully explained.[5]

Laser-Induced Fluorescence (LIF) measurements done by Williams[6] has suggested the existence of a potential hill downstream of the DCA as a possible cause of DCA erosion. Mapping of the internal plasma structure of the ion engine, specifically downstream of the DCA, is essential to understanding the cause of discharge cathode erosion. Direct measurement of plasma properties such as electron temperature, electron number density, and plasma potential would permit evaluation of the sensitivity of the discharge parameters on operating condition. Determining the dependence of the discharge plasma on operating condition would aid in determining the cause of DCA erosion and how to minimize it. The intention of this paper is to present a method for measuring electron number density and electron temperature inside the discharge chamber of an ion thruster.

Apparatus and Procedure

30 cm ion thruster background

The Functional Model Thruster (FMT) preceded the NSTAR Engineering Model Thruster (EMT) and the NSTAR Flight Thruster. The principal difference in the construction of the FMT from the EMT was the anode material. The FMT anode was aluminum while the EMT anode was spun aluminum and titanium. The second of two FMT's, FMT-2, was modified at the NASA Glenn Research Center (GRC) by Williams to allow optical access to the discharge chamber for the purpose of LIF measurements.[6] Six slots were cut into FMT-2: three slots in the plasma shield and three slots in the anode.

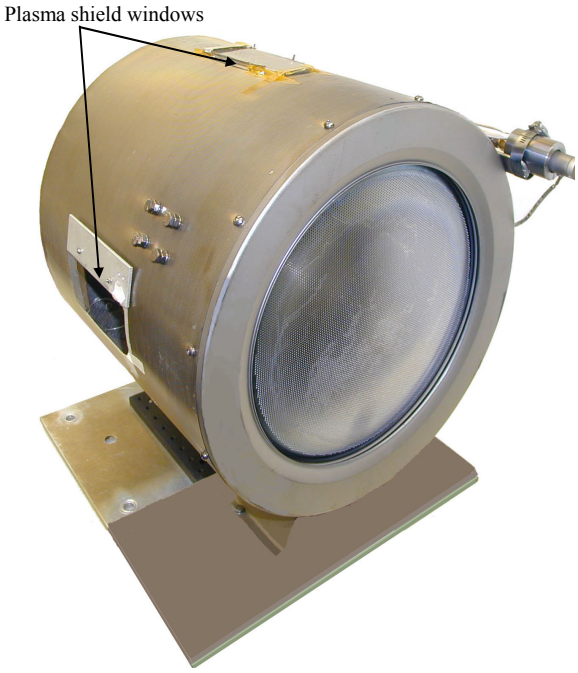

Fig. 1 – Photograph of the FMT-2 ion thruster indicating side and top plasma shield windows (bottom window not shown).

Three quartz windows covered the rectangular slots cut into the FMT-2 anode wall. These three slots, each 10.2 cm by 3.2 cm, replaced roughly twenty percent of the anode surface. The side slots of the plasma shield and anode are shown in Fig. 2.

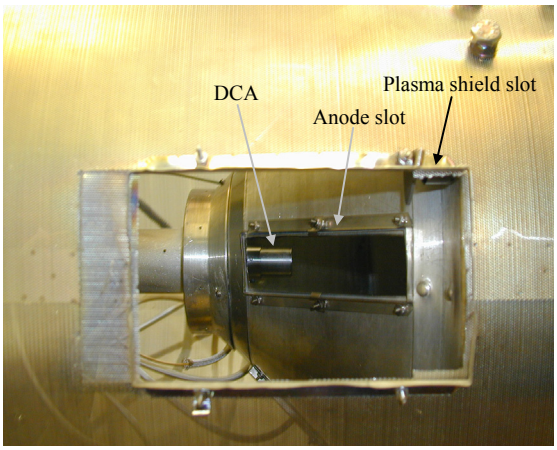

Fig. 2 - Side LIF slots and window mounts with windows removed.

The magnetic field, DCA, and geometry of the discharge chamber were identical to EMT-1's.[6] The thruster has been operated over the entire NSTAR power throttling range at GRC and PEPL illustrating comparable performance to the EMTs and flight thrusters. Williams has shown that these modifications have not altered the engine's magnetic field, discharge chamber performance, or thruster performance.[6]

New FMT-2 Modifications

Additional modifications were made to allow an electrostatic probe access inside the anode. Two of the existing windows and their mounts, one in the plasma shield side and the other in the anode side, were removed. The top and bottom windows of both the plasma shield and the anode were not altered. The criteria for selection of modifications was based on the following requirements: minimal thruster alterations, access into the discharge chamber for the probe, axial movement of the electrostatic probe, complete enclosure of the existing slot in the anode to contain the discharge plasma, and elimination of the line of sight from outside the plasma shield to the anode.

The design selected, shown in Figs. 3 and 4, was installed in FMT-2. A telescoping set of dielectric tubes minimized the protrusion of material into the discharge chamber. The inner tube retracts as the probe is moved downstream of the DCA and extends when moved towards the DCA. The plasma containment sheet consisted of 44-gauge, stainless steel held flush to the anode by a set of guides. All metal hardware installed was non-magnetic stainless steel in order to preserve the magnetic field topography. The outer telescoping tube was made of 99.8% pure alumina and the Macor inner tube was machined with a lip to create a pressure seal. The choice of two dielectric materials reduced the risk of anode to ground shorting via the plasma shield. To further insulate the anode from the plasma shield, fiberglass tape was applied to the edges of the containment sheet to minimize electric fields at the sharp edges. A rectangular piece of Macor was mounted on the inside surface of the plasma shield to avoid contact of the curling end of the containment sheet with the plasma shield.

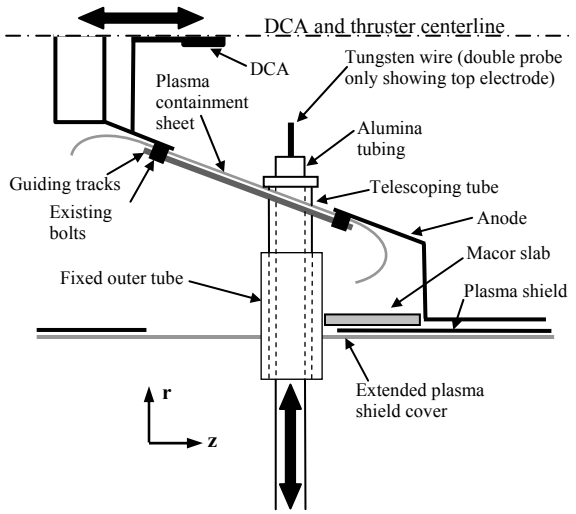

Fig. 3 - Modified FMT-2 schematic (horizontal slice).

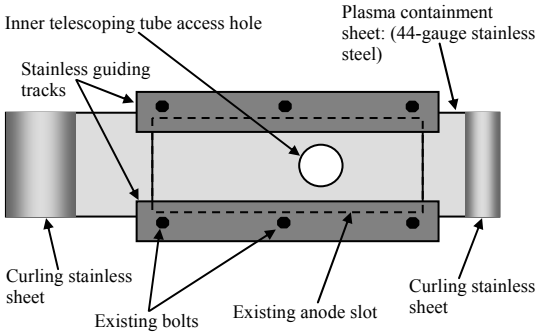

Fig. 4 – Modified FMT-2 schematic showing the side view of the hardware covering the anode side slot.

Vacuum Facility

All experiments were performed in the 6 m by 9 m Large Vacuum Test Facility (LVTF) at PEPL. Four CVI Model TM-1200 Re-Entrant Cryopumps provided a combined pumping speed of 140,000 l/s on xenon with a base pressure of 2.5×10^{-7} Torr. Chamber pressure was recorded using two hot-cathode ionization gauges. Pressure measurements from each gauge were corrected for xenon using the know base pressure on air and a correction factor of 2.87 for xenon according to,[7]

$$P_c = \frac{P_i - P_b}{2.87} + P_b \,. \qquad (1)$$

Xenon flow to the thruster was controlled using a dedicated propellant feed system provided by GRC consisting of three Edwards Mass Flow Controllers. The flow rates were calibrated over their entire operating range using a known volume technique prior to operation.

FMT-2 was mounted on a two-axis positioning system consisting of two New England Affiliated Technologies (NEAT) translational stages, which were used to move the thruster axially (absolute position accuracy of 0.15 mm). The electrostatic probe was radially positioned inside the discharge chamber using the High-speed Axial Reciprocating Probe (HARP) positioning system. The HARP system was fixed with respect to the chamber. When actuated, the probe would extend to the thruster centerline and return to its starting location just inside the inner telescoping tube.

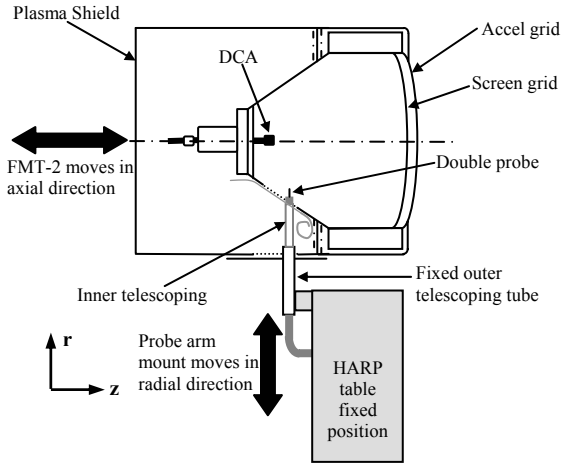

Fig. 5 - Schematic of FMT-2 orientation with respect to the HARP for probe insertion.

A 2 m by 2.5 m louvered graphite panel beam dump was positioned approximately 4 m downstream of the FMT during operation to reduce back sputtering. The thruster was operated at PEPL using a modified Skit-Pac provided by NASA GRC.

High-speed Axial Reciprocating Probe (HARP)

The probe positioning system required a highly accurate system while minimizing residence times in the plasma. These requirements led to the selection of a linear motor assembly to provide direct linear motion. The HARP system is a three-phase brushless dc servo motor consisting of a linear "U"-shaped magnet track and a "T"-shaped coil moving on a set of linear tracks. The linear encoder provided positioning resolution to 5 μm.[8] A Pacific Scientific SC950 digital, brushless servo drive was used to control the motor. A PC monitored and controlled the servo drive via a serial cable. The entire table was enclosed in a stainless steel shroud with a graphite outer skin. A probe boom mounted on an "L"-bracket extended out the side of the shroud through a slit that ran the length of the table. Residence times of the probe inside the discharge chamber were kept under 1 second to minimize probe heating and discharge plasma perturbation.

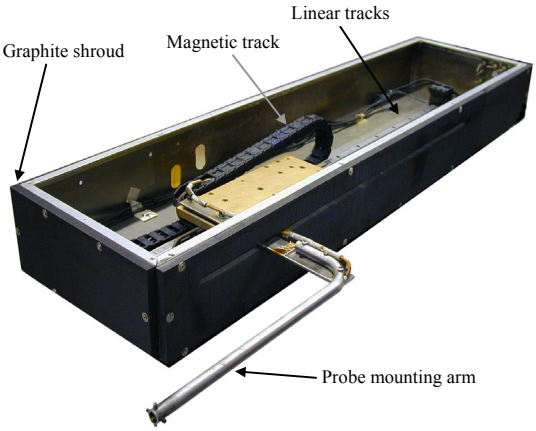

Fig. 6 - High-speed Axial Reciprocating Probe (HARP) positioning table with top cover removed (probe not installed).

Electrostatic Probe

Probes always perturb their surroundings; the extent of the perturbation is minimized by physically making the probe as small as possible. This bodes well with the need to maintain spatial resolution when making measurements. To minimize the plasma losses to the probe, the probe size was minimized while maintaining a measurable current from the predicted plasma parameters.

Several factors were taken into consideration when designing the electrostatic probe, the first being the type of probe. Unlike the single Langmuir probe, the double probe floats as a whole and thus causes less perturbation to the discharge plasma environment. The need for adequate spatial resolution and size limitations eliminated the possibility of using a triple probe. A symmetric double probe was selected because the simplicity in data analysis outweighed the benefits gained by sampling more of the I-V characteristic, accomplished using an asymmetric double probe.

The electrodes of the double probe were sized such that, for the expected electron temperature (2 – 11 eV)[9] and number densities ($1x10^{10}$ – $1x10^{12}$ cm^{-3}),[6,9] the probe would be operated in the thin sheath regime. The sheath has been estimated as five times the Debye length in the discharge plasma. In the thin sheath regime, the flux of particles entering the sheath can be calculated without considering the details about the orbits of these particles in the sheath.[10] In the thin sheath regime, the collection area of the electrode is approximated as the area of

the electrode. This approximation is justified for a large ratio of probe radius to Debye length, λ_D.

A large length to diameter ratio was chosen to minimize end effects. The gap distance, distance between the electrodes, was chosen to be at least two times larger than the expected sheath size to avoid overlapping of electrode sheaths. The size of the electrodes was chosen so that the current collected by the probe is large enough to be measured accurately, but much smaller than the discharge current as to avoid unduly perturbing the discharge plasma.

The double probe used, shown in Fig. 7, consisted of two 0.5 mm diameter cylindrical tungsten electrodes insulated from each other inside a 4.78 mm diameter 99.8% pure alumina insulator. The alumina was covered with a stainless steel tube to shield the tungsten wires. The total length of the tungsten and alumina was approximately 12 inches with 1.5 inches of alumina left unshielded towards the exposed end.

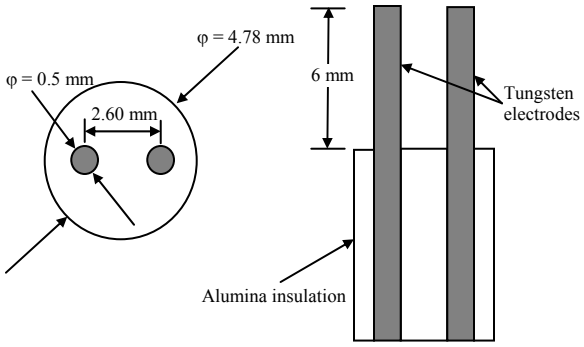

Fig. 7 - Schematic of symmetric double Langmuir probe.

Data Acquisition

As the probe is inserted into the discharge chamber, the floating potential can reach 1100 V, causing difficulty for the most electronics. Significant errors in the measured current can occur due to any appreciable stray capacitance in the circuit. Careful attention to the circuit design minimized stray capacitance and batteries were used to supply the bias voltage.[11] The battery supply consisted of twenty 6-volt lantern batteries connected in series. A potentiometer was attached to the battery output in order to adjust the bias voltage output.

The double probe circuit had been used previously to make similar measurements inside the discharge channel of a Hall Thruster.[11] The double probe circuit was built around two Analog Devices AD210 isolation amplifiers. These amplifiers are capable of handling up to 2500 volts of common mode voltage and provide an input impedance of $1x10^{12}$ Ω. The low impedance output (1 Ω maximum) was connected to a digital oscilloscope that, when triggered off the probe position, recorded the data and saved it to a computer. Figure 8 illustrates the double probe circuit.

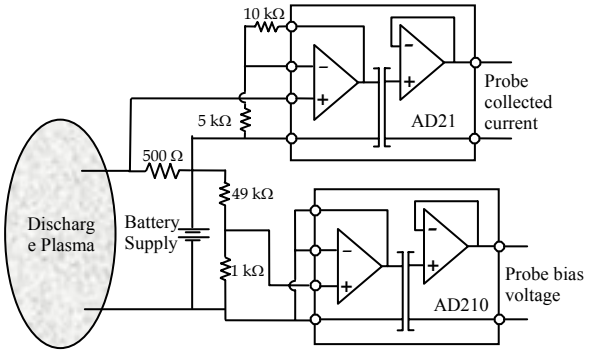

Fig. 8 - Double probe circuit electric diagram.

The outputs of the isolation amplifiers were calibrated with known currents and bias voltages over their entire operating ranges. A digital sourcemeter was connected across the two electrodes to simulate the collected current of the probe. The output of the probe current shunt was then measured as a function of known supplied current, resulting in a linear calibration curve. A similar calibration of the bias voltage output was done by applying known bias voltages between the electrodes and measuring the probe bias voltage output.

The probe position, FMT-2 discharge current, double probe collected current, and double probe bias voltage are all recorded during the sweep as a function of time. From this information, the discharge current, probe collected current, and probe bias voltage can be calculated as a function of probe position. Figure 9 illustrates a sample radial sweep taken 2.6 mm downstream of the DCA. The discharge current and voltage were 10.87 A and 25.40 V, respectively, with a probe bias of 6 volts.

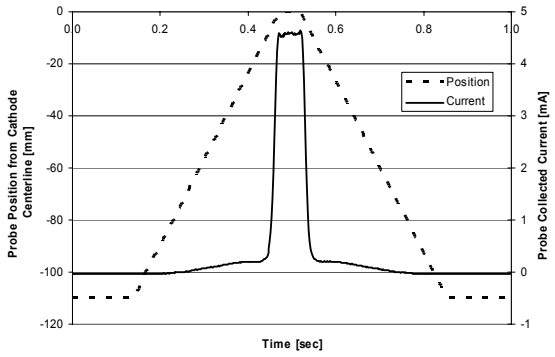

Fig. 9 - Representative radial sweep at 2.6 mm downstream of the DCA (10.87 A-25.40 V).

At each thruster operating condition and fixed bias voltage, the probe position and collected current were measured as a function of time during the radial sweep into the discharge chamber. The bias voltage was then adjusted and the probe swept into the discharge chamber again. The resulting data were later reassembled to obtain the current-voltage characteristic of the double probe at each location in the radial sweep. Only data taken on the "in sweep" of the probe were used. Figure 10 represents a typical current-voltage characteristic taken 2.6 mm downstream of the DCA at a radial location of 10 mm from the DCA centerline. The discharge cathode operating conditions were again 10.87 A and 25.40 V. The collected current continues to increase, with increasing bias voltage, past the "knee" due to sheath expansion.

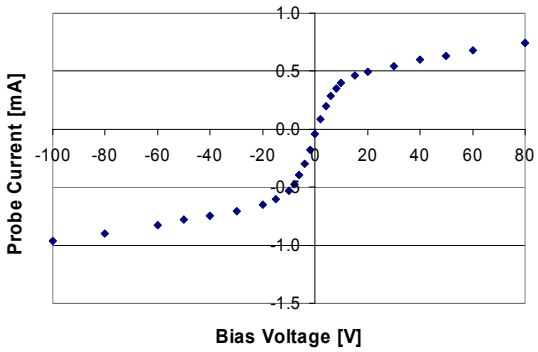

Fig. 10 - Typical I-V characteristic curve 2.6 mm downstream of DCA, 10 mm from DCA centerline (10.87 A-25.40 V).

Data Analysis

From the I-V characteristic curves, linear curve fits were made to the linear region near the origin. The ion saturation current was estimated as the probe current collected just past the "knee" in the characteristic. The slope of the linear region, the ion saturation current, the collection area of the probe, and appropriate constants are used to determine the electron temperature and number density according to Eqs. 2 and 3.[12]

$$T_e = \frac{i_{ion,sat} e}{2k\left(\left.\frac{di}{dV}\right|_{V=0}\right)} \tag{2}$$

$$n_e = \frac{i_{ion,sat}}{eA_p}\sqrt{\frac{M_{Xe}}{kT_e}} \tag{3}$$

As is the case with any Langmuir probe measurements, the electron temperature is inferred from the ion saturation current and the slope of the characteristic in the electron retarding region. The number density is calculated from the ion saturation current and electron temperature calculation. As a result any errors in estimating the ion saturation current or the slope of the characteristic lead to errors in the electron temperature, but are compounded in the calculation of the electron number density. Thus the error in plasma parameters can be significant. Typical estimates for the error in electron temperature and electron number density are 20% and 50%, respectively.

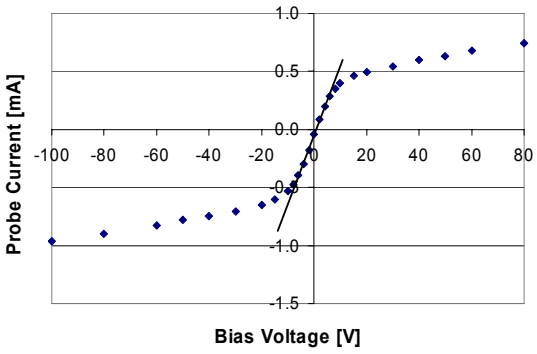

Fig. 11 - Typical linear curve fit to the linear region of the characteristic.

Results and Discussion

For these initial experiments, radial sweeps were taken at an axial location of 2.6 mm downstream of the DCA over four different operating conditions. Table A.1 in the appendix lists the calculated plasma parameters and Debye lengths. The test was unexpectedly shutdown due to the failure of the isolation amplifier (mounted in the chamber) that measured the probe collected current. This occurred before the probe could be moved downstream of the DCA to take additional radial sweeps. Time constraints prohibited further testing.

Since the focus of this investigation is discharge cathode phenomena, the primary thruster operating conditions of concern are the discharge current and voltage. For each operating condition, the discharge current, neutralizer keeper current, screen grid voltage, and acceleration grid voltage were set to their corresponding values in the NASA Throttling Conditions (TH Level) Tables. The main anode flow rate and discharge cathode flow rate were adjusted until both the discharge voltage and beam current matched their respective values for the indicated NASA TH Level. All of the values corresponding to

NASA TH Levels could not be met and as a result the operating conditions of the FMT-2 are referred to as Discharge Conditions (DC Levels) instead of TH Levels. Below is an abbreviated list of telemetry focusing only upon the discharge parameters. For a complete listing of thruster parameters see Tables A.2 and A.3 in the appendix for experiment DC Level parameters and NASA TH Level parameters, respectively.

Table 1 - Reference NASA throttling parameters

TH Level	Vd	Jd	Main flow	Disch. cathode flow
	V	A	sccm	sccm
TH 4	25.61	6.05	8.30	2.47
TH 8	25.10	8.24	14.41	2.47
TH 12	25.40	10.87	19.86	2.89
TH 15	25.14	13.13	23.43	3.70

Table 2 - Experiment discharge parameters

DC Level	Vd	Jd	Main flow	Disch. cathode flow
	V	A	sccm	sccm
DC 4	25.62	6.05	10.9	2.34
DC 8	25.05	8.24	17.0	1.86
DC 12	25.36	10.87	20.3	3.51
DC 15	25.13	13.13	23.3	3.71

Figures 12 and 13 illustrate the calculated plasma parameters. The number densities fall within the expected range with values from 8.9×10^{10} - 2.1×10^{12} cm^{-3} over all operating conditions and radial locations investigated. As expected, the maximum number density for each operating condition occurs along the DCA centerline and falls off by at least an order of magnitude 10 mm away. The measured number densities are well within the range required to cause DCA erosion from singly-ionized xenon that is consistent with the 8200 hour wear test results, as stipulated by Williams.[2,6]

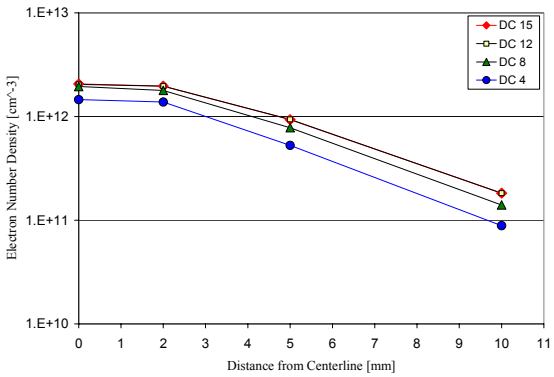

Fig. 12 - Electron number density calculations

The electron temperatures also fall within the predicted range with values from 3.2 - 4.8 eV over all operating conditions and radial locations considered. There are no observable trends in the radial electron temperature data as any possible trends can be dismissed due to the uncertainty in the measurements.

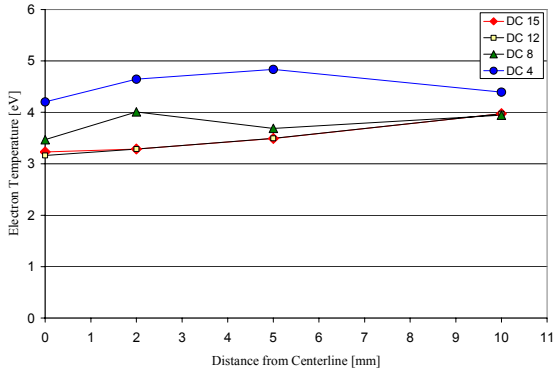

Fig. 13 - Electron temperature calculations

Error Analysis

Traditional estimates of the error in electrostatic probe measurements are typically 50% for electron number density and 20% for electron temperature. While these errors are large it is believed that the relative error between two measurements using identical setups is not this high.

There are several different probe regimes that depend upon the fundamental lengths in the plasma. Care was taken to ensure that over the domain of interest, the probe radius is much larger than the Debye length. This ensures that ion orbits are negligible when interpreting the probe characteristic.[12] The maximum Debye length calculated from the data was 0.05 mm. This gives a ratio of probe radius to Debye length of five. The Debye length grows significantly as the distance from the discharge cathode is

increased since the electron temperature is roughly constant while the electron number density falls off rapidly. With the maximum Debye lengths occurring 10 mm away from the DCA centerline, there is less confidence in these data points as the thin sheath theory does not strictly apply. However, for the data at 5, 2, and 0 mm, the maximum Debye length is 0.02 mm resulting in a probe radius to Debye length of approximately 12. Thus, thin sheath theory is applicable for these data points.

Under normal operation of a double probe, it is important that the electrode sheaths are not overlapping. Symmetric double probe theory assumes that the electrodes are identical and that they are close enough together that the plasma is identical at both positions. The current collected from one electrode is emitted by the other, however the two electrodes need to be "independent" from each other in that the plasma being measured is the only connection between the two. Overlapping of the electrode sheaths results in a means of "communication" between the two probes, which invalidates the double probe theory used. Estimating the sheath thickness, five times the Debye length, results in a maximum sheath thickness for the entire test of roughly 0.3 mm. With a gap between electrodes of 2.1 mm there is approximately 1.5 mm separating the sheaths for the worst case scenario.

To ascertain the perturbation introduced by the probe, measurement of the discharge current is recommended. It was intended to monitor discharge current during probe insertion, however, the existing measurement of discharge current incorporates a shunt floating at high voltage. Possible shorting of the discharge current shunt through the oscilloscope prohibited this measurement and due to time constraints another method of monitoring the discharge current, either via a Hall sensor or a shunt with an isolation amplifier, was not incorporated. As a result the perturbation to the discharge plasma can only be estimated by monitoring discharge current during probe insertion without beam extraction where the plasma is not at a high voltage.

Prior to high voltage operation with beam extraction, the discharge cathode was operated with similar discharge currents and voltages without beam extraction. For the cases without beam extraction, the discharge current was monitored via the current shunt. Shorting through the oscilloscope did not occur because the high voltage was not on, thus the shunt had not floated up to approximately 1100 V as would be the case with beam extraction. During these cases, the probe was overshooting the discharge cathode centerline causing substantial perturbations; however, data was only taken during the "in sweep" to avoid the incurred error due to the overshoot. Figures 14 and 15 illustrate the perturbation to the discharge current for probe insertion without beam extraction at discharge conditions of 6.05 A, 24.5 V and 13.13 A, 21 V, respectively. The 20 volts bias case is illustrated because all of the current-voltage characteristics had passed the "knee" in the curve around or prior to the 20 volts bias. Thus, the maximum discharge current variations, which will affect the calculation of plasma parameters, occur at the 20 volts bias. The maximum percent variation of discharge current, occurring for the 6.05 A case, is roughly six percent. It should be noted that the probe used for the tests without beam extraction had a significantly larger collection area than for the data presented (with beam extraction). Thus, the perturbation without beam extraction should be higher than the actual perturbation with beam extraction. During the discharge-only tests, the probe consisted of two 1.12 mm diameter electrodes 8.8 mm in length (more than three times the collection area than the beam extraction probe).

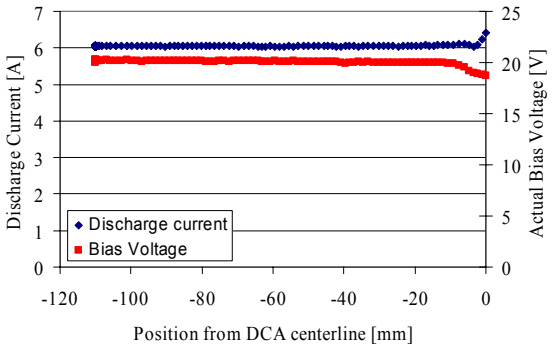

Fig. 14 - Sample discharge and bias voltage perturbation (20 V bias, 6.05 A, 24.5 V shown) without beam extraction for 1.12 mm diameter electrodes

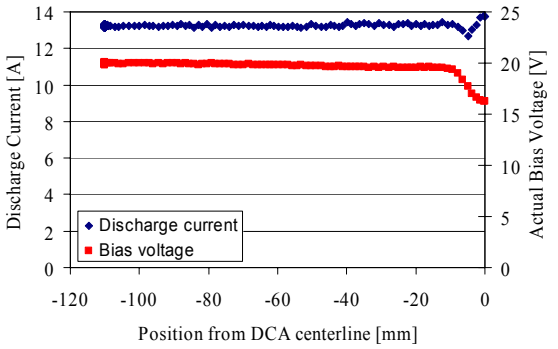

Fig. 15 - Sample discharge and bias voltage perturbation (20 V bias, 13.13 A, 25 V shown) without beam extraction for 1.12 mm diameter electrodes

Another measure of the probe perturbation is the ratio of the collected current to the discharge current. The maximum ion saturation current collected was on the order of milli-amperes. The minimum discharge current was approximately 6 A. Thus the collected current was at most 0.3 percent, using the maximum collected current for the entire test operating conditions and minimum discharge current.

Batteries were used to supply the bias voltage to minimize the stray capacitance of the double probe circuit. For each bias voltage set, the bias voltage was measured at the electrodes using the double probe circuit. When analyzing the data, a problem with the oscilloscope channel monitoring the bias voltage was found that prevented measurement of the actual bias voltage as the probe was inserted. If the current limit of the battery source is approached, the bias voltage can sag, adding to the uncertainty in the measurements. The variance in bias voltage as the probe was inserted can be estimated from data taken for comparable discharge operating conditions without beam extraction. Figures 14 and 15 illustrate the variation of bias voltage of a probe during insertion without beam extraction at discharge conditions of 6.05 A, 24.5 V and 13.13 A, 25 V, respectively. Again it should be noted that the probe used during discharge-only tests consisted of 1.12 mm diameter electrodes with a collection area of more than three times that of the electrode actually used for data collection.

Figure 15 illustrates a noticeable variation of the bias voltage as the probe is inserted into the discharge chamber. As much as 19% variation from the set 20 volts bias was observed. The decreased area (by a factor of three) of the probe used for beam extraction data will result in a decrease in the magnitude of voltage sag. It is not clear how much reduction in voltage sag occurred for the smaller probe or if this smaller voltage sag was even noteworthy. The 13.13 A condition is a worst case since at the highest discharge current, and therefore highest number density, more current will flow from one electrode to the other and hence more current will be drawn from the batteries. Had the actual bias voltage been recorded during the experiment with beam extraction, the variation in bias voltage could have been corrected for. This observation tends to place less confidence in the higher discharge current measurements.

Conclusions

A method of interrogating the discharge chamber plasma has been demonstrated. During the initial set of radial sweeps valuable lessons were learned and preliminary discharge plasma parameters were calculated for four thruster operating conditions. The data were found to agree with estimates for both electron temperature and number density. From this preliminary data, improvements can be made to minimize discharge current perturbation and increase the accuracy of the electrostatic probe measurements.

Future Work

The present work lays the foundation for higher spatial resolution and reduced error double probe measurements. The preliminary plasma parameter data collected will allow better double probe construction and an overall more specialized system.

Future tests will take double probe data over a two-dimensional range of locations downstream of the DCA. Incorporation of a Hall probe or the use of isolation amplifiers to record the discharge current is essential to monitor the perturbation introduced by the probe to the discharge plasma. Correction of oscilloscope problems will allow the measurement of bias voltage as a function of probe position in order to monitor and adjust for any minor amount sagging of bias voltage. More importantly, a different battery source capable of handling the current requirements will be employed to greatly reduce the voltage sag. The scientific graphing package Igor will be used to extract discharge plasma parameters from current-voltage characteristics using a more repeatable and accurate least-squares fit of the theoretical hyperbolic tangent curve to the I-V characteristic for symmetric double probe data.[12,13]

After completing double probe measurements, an emissive probe will be employed to map the plasma potential inside the discharge chamber. This could validate or rule out the existence of a potential hill, which has been proposed as a possible explanation of DCA erosion.

Acknowledgements

We would like to thank Dr. George Williams and Dr. James Haas whose exceptional work at the University of Michigan has laid the foundation for this research. They have gone beyond the call of duty to offer direction, answer questions, and lend assistance.

We would also like to thank the entire research group at PEPL who have been instrumental in this investigation.

We would also like to thank the NASA Glenn Research Center (GRC) for their financial support through research grant NAG3-2216 and for use of their equipment. We would especially like to acknowledge Dr. Matt Domonkos (grant monitor), Dr. John Foster, and Dr. George Williams who have been the principal contacts at NASA GRC and offered assistance when called upon.

References

[1] http://nmp.jpl.nasa.gov/ds1/gen/mission.html

[2] Polk, J. E., et al., "An Overview of the Results from an 8200 Hour Wear Test of the NSTAR Ion Thruster," AIAA Paper No. 99-2446, *35th AIAA / ASME / SAE / ASEE Joint Propulsion Conference*, Los Angeles, CA, June 1999.

[3] Williams, G. J., et al., "Characterization of FMT-2 Discharge Cathode Plume," IEPC Paper No. 99-104, *26th International Electric Propulsion Conference*, Ketakiushu, Japan, Oct. 1999.

[4] Anderson, J. R., et al, "Performance Characteristics of the NSTAR Ion Thruster During and On-Going Long Duration Ground Test," IEEE Paper No. 8.0303, *IEEE Aerospace Conference*, Big Sky, MT, Mar. 2000.

[5] Domonkos, M. T., Foster, J. E., Patterson, M. J., "Investigation of Keeper Erosion in the NSTAR Ion Thruster," IEPC Paper No. 01-308, *27th International Electric Propulsion Conference*, Pasadena, CA, Oct. 2001.

[6] Williams, G. J., *The Use of Laser-Induced Fluorescence to Characterize Discharge Cathode Erosion in a 30 cm Ring-Cusp Ion Thruster*, Ph.D. Dissertation, University of Michigan, 2000.

[7] Hofer, R. R., Peterson, P. Y., Gallimore, A. D., "Characterizing Vacuum Facility Backpressure Effects on the Performance of a Hall Thruster," IEPC Paper No. 01-045, *27th International Electric Propulsion Conference*, Pasadena, CA, Oct. 2001.

[8] Haas, J. W., et al, "Development of a High-Speed, Reciprocating Electrostatic Probe System for Hall Thruster Interrogation," *Review of Scientific Instruments*. Vol. 71, No. 11, pp. 4131-4138, Nov. 2000.

[9] Beattie, J. R., et al, "Mercury Ion Thruster Technology Final Report," Hughes Research Labs. Feb. 1983 – Oct. 1984.

[10] Hershkowitz, N., "How Langmuir Probes Work," *Plasma Diagnostics*. Nuclear Engineering and Engineering Physics Department, University of Wisconsin-Madison, 1989.

[11] Haas, J. W., *Low-Perturbation Interrogation of the Internal and Near-Field Plasma Structure of a Hall Thruster using a High-Speed Probe Positioning System*, Ph.D. Dissertation, University of Michigan, 2001.

[12] Mott-Smith, H., and Langmuir, I. *Physics Review*, 28, 727, 1926.

[13] Smith, B. A., et al, "Improvements to Floating Double Probes for Time-resolved Measurements in Pulsed RF Plasmas," *Review of Scientific Instruments*, Vol. 69, No. 3, pp 1372, Mar. 1998.

Appendix

Table A.1 - Calculated plasma parameters with beam extraction.

DC Level	Distance from Centerline [mm]	T_e [eV]	n_e [cm^{-3}]	Debye Length, λ_D, [mm]
15	0	3.2	2.1E+12	0.009
15	2	3.3	2.0E+12	0.010
15	5	3.5	9.4E+11	0.014
15	10	4.0	1.8E+11	0.035
12	0	3.2	2.0E+12	0.009
12	2	3.3	2.0E+12	0.010
12	5	3.5	9.4E+11	0.014
12	10	4.0	1.8E+11	0.035
8	0	3.5	2.0E+12	0.010
8	2	4.0	1.8E+12	0.011
8	5	3.7	7.8E+11	0.016
8	10	3.9	1.4E+11	0.039
4	0	4.2	1.5E+12	0.013
4	2	4.6	1.4E+12	0.014
4	5	4.8	5.3E+11	0.022
4	10	4.4	8.9E+10	0.052

Table A.2 - Thruster telemetry for Discharge Conditions for plasma parameter measurement with beam extraction.

DC Level	V_b	J_b	V_a	J_a	V_d	J_d	V_{nk}	J_{nk}	Main flow	Disch. cathode flow	Neutralizer cathode flow	V_g (Neutr-grnd coupling)	Pressure
	V	A	V	mA	V	A	V	A	sccm	sccm	sccm	V	Torr
DC 4	1100	0.71	-150.0	2.24	25.62	6.05	18.00	2.0	10.9	2.34	4.40	9.47	2.4E-06
DC 8	1100	1.10	-180.0	4.19	25.05	8.24	17.51	1.5	17.0	1.86	4.40	13.33	3.1E-06
DC 12	1102	1.49	-180.1	6.19	25.36	10.87	15.99	1.5	20.3	3.51	4.40	13.15	3.9E-06
DC 15	1101	1.76	-180.3	7.88	25.13	13.13	15.48	1.5	23.3	3.71	4.40	13.03	4.2E-06

Table A.3 - Telemetry for NASA Throttling Levels for DS1.

TH Level	V_b	J_b	V_a	J_a	V_d	J_d	V_{nk}	J_{nk}	Main flow	Disch. cathode flow	Neutralizer cathode flow
	V	A	V	mA	V	A	V	A	sccm	sccm	sccm
TH 0	650	0.51	-150	1.443	25.20	4.29	17.36	2.0	5.98	2.47	2.40
TH 1	850	0.53	-150	1.486	25.40	4.69	17.07	2.0	5.82	2.47	2.40
TH 2	1100	0.52	-150	1.463	25.40	5.12	16.79	2.0	5.77	2.47	2.40
TH 3	1100	0.61	-150	1.673	25.40	5.57	16.52	2.0	6.85	2.47	2.40
TH 4	1100	0.71	-150	1.927	25.61	6.05	16.26	2.0	8.30	2.47	2.40
TH 5	1100	0.81	-150	2.204	25.40	6.56	16.01	2.0	9.82	2.47	2.40
TH 6	1100	0.91	-150	2.505	25.40	7.09	15.77	2.0	11.33	2.47	2.40
TH 7	1100	1.00	-150	2.795	25.40	7.65	15.54	2.0	12.90	2.47	2.40
TH 8	1100	1.10	-180	3.139	25.10	8.24	15.32	1.5	14.41	2.47	2.40
TH 9	1100	1.20	-180	3.507	25.40	8.86	15.11	1.5	15.98	2.47	2.40
TH 10	1100	1.30	-180	3.898	25.83	9.50	14.90	1.5	17.22	2.56	2.49
TH 11	1100	1.40	-180	4.312	25.40	10.17	14.71	1.5	18.51	2.72	2.65
TH 12	1100	1.49	-180	4.704	25.40	10.87	14.52	1.5	19.86	2.89	2.81
TH 13	1100	1.58	-180	5.115	25.40	11.60	14.35	1.5	20.95	3.06	2.98
TH 14	1100	1.67	-180	5.544	25.40	12.35	14.18	1.5	22.19	3.35	3.26
TH 15	1100	1.76	-180	5.993	25.14	13.13	14.02	1.5	23.43	3.70	3.60